Optimal multi-objective integration of photovoltaic, wind turbine, and battery energy storage in distribution networks

Mohammad Rasol Jannesar[1], **Alireza Sedighi**[1,*], **Mehdi Savaghebi**[2], **Amjad Anvari-Moghaddam**[3], and **Josep M. Guerrero**[3]

[1] *Department of Electrical engineering, Yazd University, Yazd, Iran*
[2] *Electrical Engineering Section, The Mads Clausen Institute, University of Southern Denmark, Odense, Denmark*
[3] *Department of Energy Technology, Aalborg University, Aalborg, Denmark*
[*] *Corresponding author: sedighi@yazd.ac.ir*

Manuscript received 29 January, 2020; revised 27 April, 2020, accepted 29 April, 2020. Paper no. JEMT-2001-1227.

In recent years, grid integration of renewable energy sources (RES) and battery energy storage systems (BESS) has been rising rapidly. Many economic, technical, and environmental benefits can be gained with the integration of RES and BESS into the distribution network. Optimal decisions must be considered the trade-offs between two or more conflicting objectives, therefore, in this paper, these benefits are associated with a multi-objective function that consists of energy price arbitrage, transmission access fee, energy losses, power quality (voltage regulation), and environmental emissions. In this paper, it is assumed that the distribution system operator (DSO) has got the ownership of RES and BES. The placement, sizing, and operation of RES and BESS are optimized by the combination of a genetic multi-objective solver (GMOS) with linear programming. The simulation results using IEEE 33-bus distribution test system show that by using the proposed method, the net benefit is appropriate, energy losses are reduced, voltage magnitude is pushed within the limit, and environmental emissions are decreased.

keywords: *Battery energy storage, Multi-objective, Optimal integration, Photovoltaic, Wind Turbine.*

http://dx.doi.org/10.22109/jemt.2020.217725.1227

1. INTRODUCTION

Renewable energy sources (RES) penetration has been increasing due to the global energy crises and environmental concerns of fossil fuel-based electricity generation [1]. Reverse power flow to the transmission network, losses, and some power quality problems, for instance, over-voltage may occur when RES and battery energy storage systems (BESS) are placed without any optimal planning or RES penetration is very high [2]. On the other hand, in rural distribution networks, because of the high R/X ratio, voltage magnitude on buses far from the transformers may go below the allowable limit when end-use demand is increased. Therefore, the distribution system operator (DSO) should monitor such power quality problems to decrease under-voltage by methods such as network equipment upgrades, which could be relatively expensive. However, by optimal planning and operation of RES and BESS, DSO can postpone the network expansion options such as reconductoring [3]. Furthermore, by optimal integration of RES and BESS, operation cost, environmental emissions, and energy losses are reduced. In addition, DSO can schedule BESS operation to mitigate disadvantages originated from high penetration of customer-owned RES [4]. Therefore, economic, environmental, technical, and socio-political factors could be improved [5].

In this context, special focus has been given to optimal planning and operation of RES and energy storage system (ESS) over the past couple of years.

Some previous researchers have performed only the optimal operation of RES and ESS. For example, the joint optimal operation of photovoltaics (PVs), electric vehicles, and ESSs is proposed in [6] to increase the local utilization of renewable energy. Authors of [7] proposed a model to find optimal daily operation scheduling of a hybrid system to minimize the use of the diesel generator, whereas maximizing the utilization of the wind turbine (WT), PV, and pumped hydro storage system.

There are many kinds of research addressing only the optimal planning of RES and ESS. As one of the first works in this area, optimal planning of PV, BESS, and distributed static compensator is performed in [8] to improve technical, economic, reliability, and environmental aspects in the distribution system. Authors of [9] presented a joint optimal allocation methodology of RES and distributed ESS to achieve economic benefits for a distribution company (DISCO). In [10], optimal sizing and sitting of ESS and distributed generation (DG) are addressed from the perspective of the DSO to minimize the total investment cost, whereas maximizing the payoff by offering transacted services in the distribution market.

In some recent works, optimal planning (without placement) and operation of RES and ESS are studied. For instance, a two-stage optimal energy management system is designed for microgrids with RESs and ESSs [11]. In [12], optimal sizing and energy scheduling of PV and BESS are presented based on the highest system net present value to decrease peak consumption of the grid. A model is designed in [13] to size a hybrid RES with BESS that can be used to supply electrical load demands with the lowest investment cost. In [14], a multi-criteria approach is presented to design a hybrid renewable energy system considering the loss of power supply probability, total energy loss, and the power difference between generation and storing capacity.

In [15], place and capacity of ESS and DGs are determined to maximize the profit of DISCO. The transmission access fee is not considered in [15]. Authors of [16] proposed a new risk-based method to determine the optimal location and capacity of ESS units and wind turbines simultaneously. Authors of [17] presented a two-level planning approach to plan the installation of ESS and DG on the network and determine an hourly optimal operation strategy for ESS and DG to minimize annual operation cost of distribution network subject to security constraints. Optimal sizing of PV and BESS is performed in [18] to minimize the investment cost while guarantying the desired level of reliability in the energy supply. Environmental emission is not considered in [17, 18]. In [19], optimal planning and operation of BESS are performed, but, the multi-objective study is not taken into account. Authors of [20] presented a stochastic scheduling of thermal units with coordination of WT and ESS considering security constraints. In [21], a new method is suggested to determine the optimal capacity of WT and ESS for investment deferral of sub-transmission substations.

Some other works study multi-objective optimization without considering environmental emission. For instance, optimal multi-objective sizing and sitting of RES, electric vehicle charging stations, and ESSs are presented in [22] considering the time-varying nature of RES and load consumption. Authors in [23] have addressed the optimal multi-objective sitting and sizing of a BESS with WT and PV in a distribution system to reduce losses and cost, improve the voltage profile, and extend the lifespan of the batteries. A multi-objective based genetic algorithm approach was used to size a multi-source PV/WT with hybrid ESS to minimize the total cost of electricity and loss of power supply probability [24]. In [25], multiple configurations and placement of step-voltage regulators, capacitor banks, BESS, and WT are proposed to improve energy loss, voltage deviation, and cost. In [26], optimal multi-objective sizing of RES and BESS is presented to minimize the annualized cost of the system and maximize the autonomy from the main grid. In another work, a method is presented for optimizing battery capacity and operation parameters of grid-connected PV-BESS with a multi-objective genetic algorithm [27]. The optimal energy management of RES and ESS is proposed in [28] to solve an environmental/economic bi-objective optimization problem. A multi-objective optimal design of a hybrid renewable energy system is presented in [29] considering technical, economic, and social objectives. In these papers ([26–29]), energy losses are not considered.

This paper extends the works reported in the literature review by presenting a multi-objective function consisting of economic benefit, environmental (CO2 emission reduction), and technical objectives as well as the capital, operation, maintenance, and replacement costs of RES and BESS. The main contributions of the present paper are summarized below:

- Considering both optimal planning and operation (extension of [6–10]).
- In planning, in addition to sizing, the placement is performed (extension of [11–14]).
- For economic objective, increasing energy arbitrage and decreasing transmission access fee (extension of [15]) are simultaneously taken into account.
- The technical objectives cover voltage magnitude and reverse power flow control and also energy loss (extension of [26–29]). For this purpose, the reduction of energy losses is modeled as one of the terms in the objective function. On the other hand, voltage magnitude and reverse power flow control are modeled as constraints.
- A new method including the combination of the genetic multi-objective solver (GMOS) and linear programming is used for solving this function. This solver is first applied to obtain the Pareto-optimal solutions, and then the proper solution is identified, with respect to economic, environmental, and technical objectives.

2. MULTI-OBJECTIVE FUNCTION MODELING

In a restructured power market with dynamic price model, energy price differs for different hours of the day. Therefore, the BESS owner (which is DSO in our study) can purchase energy from the market when the energy price is low to charge the BESS. When the energy price is relatively higher, this energy could be sold to the power market [30]. Furthermore, DSO should pay the transmission access fee to use transmission equipment. RES and BESS produce energy locally, so transmission access fee is decreased. In addition, the use of conventional power plants increases environmental emissions, whereas by utilizing RES such as WT and PV in the network, the environmental emission could be reduced. Moreover, based on optimal placement, sizing, and operation of RES and BESS in the distribution network, energy losses can be reduced, and voltage regulation can be improved.

In this paper, a multi-objective function is defined by DSO for optimization analysis where optimal decisions need to be taken considering the trade-offs between two or more conflicting objectives. In the following, economic, environmental, and technical objectives, RES and BESS cost, as well as constraints are defined.

A. The benefit of energy price arbitrage

In an electricity market with dynamic pricing, energy price rates are set hourly. This implies that BESS could be respectively charged and discharged in low-price and high-price periods to meet the economic objectives. In some power markets, because of government incentives and subsidies, the selling rate of RES and BESS power production is higher than energy price rates. Since the selling rate of RES and BESS power production is different for each power market, in this paper, it is assumed that power productions of RES and BESS are sold in the power market by energy price rates. These benefits are expressed as (1):

$$ARB_{BEN} = \sum_{i=1}^{24} \left(\left(P_i^+ - P_i^-\right) + P_i^{WT} + P_i^{PV} \right) pr_{en,i} \tag{1}$$

where ARB_{BEN} is the arbitrage benefit. P_i^+ and P_i^- are discharge and charge power of BESS in the i^{th} hour. P_i^{WT} and P_i^{PV} are the average hourly power of WT and PV in the i^{th} hour, respectively. $pr_{en,i}$ is the average hourly energy price in i^{th} hour modified from the New York Independent System Operator market [31].

B. The benefit of transmission access fee

In a restructured power system, DSO should pay the transmission access fee to use transmission equipment. Transmission access fee varies at different hours of a day. BESS can be charged and discharged in low and high access fees, respectively. On the other hand, when RES is connected to a distribution system, DSO should not pay transmission access fee for the energy production of RES. These benefits are shown in (2):

$$TRANS_{BEN} = \sum_{i=1}^{24} \left(\left(P_i^+ - P_i^-\right) + P_i^{WT} + P_i^{PV} \right) pr_{trans,i} \tag{2}$$

where $pr_{trans,i}$ is the average hourly transmission access fee in i^{th} hour [31].

C. Environmental emissions reduction

Due to the different greenhouse emission rates of conventional power plants, the emission rate differs in 24 hours of the day. BESS can be charged and discharged in low and high greenhouse gas emission rates, respectively. On the other hand, RES is a green power plant; therefore, RES and BESS can reduce air pollution. This objective is shown in (3):

$$ENV_{OBJ} = \sum_{i=1}^{24} \left(\left(P_i^+ - P_i^-\right) + P_i^{WT} + P_i^{PV} \right) EMI_{rate,i} \tag{3}$$

where $EMI_{rate,i}$ is average hourly CO_2 emission rate of conventional power plants in i^{th} hour [32].

D. Loss reduction

Optimal placement, sizing, and operation of RES and BESS could reduce energy losses because load demand is supplied by RES and BESS that produce power locally instead of receiving power through distribution transformers. This technical objective models hourly energy loss reduction as discussed in [19] and shown in (4):

$$LOSS_{OBJ} = LOSS_{old} - LOSS_{new} \tag{4}$$

where $LOSS_{old}$ and $LOSS_{new}$ are energy loss before and after optimization, respectively.

E. Capital and maintenance cost

RES and BESS costs consist of investment and operation costs. Investment costs of BESS, WT, and PV are shown in (5):

$$\begin{aligned} C_{RES\&BESS} &= C_{S,B} S_{max,B} + C_{WS,B} S_{W\,max,B} + C_{S,WT} P_{max,WT} \\ &+ C_{S,PV} P_{max,PV} \end{aligned} \tag{5}$$

where $C_{S,B}$ and $C_{WS,B}$ show the costs related to power and energy capacity of the battery, respectively. $S_{max,B}$ indicates maximum apparent power and $S_{W\,max,B}$ is the optimal energy capacity of BESS. $C_{S,WT}$ and $C_{S,PV}$ are the capital cost of WT and PV, respectively. $P_{max,WT}$ and $P_{max,PV}$ are respectively maximum power capacities of WT and PV.

The operation, maintenance, and replacement costs are related to maximum power. These costs are shown in (6):

$$C_{O\&M\&REP} = C_{O\&M,B} + C_{O\&M\&REP,WT} + C_{O\&M\&REP,PV} \tag{6}$$

where $C_{O\&M,B}$ is the operation and maintenance costs of BESS and $C_{O\&M\&REP,WT}$ and $C_{O\&M\&REP,PV}$ are operation, maintenance, and replacement costs of WT and PV, respectively.

In the current paper, the battery is charged and discharged once a day. Due to the planning period (20 years) and cycle life (12000 [33]) of battery used in this paper (vanadium redox battery), the replacement cost of the battery is zero. These costs can be introduced as (7)-(9):

$$C_{O\&M,B} = \left(C_{Mf\,B} + C_{Mv\,B}\right) S_{max,B} \tag{7}$$

$$C_{O\&M\&REP,WT} = \left(C_{Mf\,WT} + C_{Mv\,WT} + C_{REP_{COST},WT}\right) P_{max,WT} \tag{8}$$

$$C_{O\&M\&REP,PV} = \left(C_{Mf\,PV} + C_{Mv\,PV} + C_{REP_{COST},PV}\right) P_{max,PV} \tag{9}$$

where C_{MfB} represents operating and maintenance cost for power convertor system and C_{MvB} is the cost of electrical losses to maintain the power convertor system and battery in hot standby intervals. Also, C_{MfWT} and C_{MvWT} are fixed and variable operating and maintenance specific costs of WT; C_{MfPV} and C_{MvPV} are the same costs for PV. Also, $C_{REP_{COST},WT}$ and $C_{REP_{COST},PV}$ are the replacement costs of WT and PV, respectively.

Maximum apparent power ($S_{max,B}$) and optimal energy capacity of BESS ($S_{W\,max,B}$) are calculated as:

$$\begin{aligned} S_{max,B} &= \sqrt{\left(P_{max,B}\right)^2 + \left(Q_{max,B}\right)^2} \\ S_{W\,max,B} &= \sqrt{\left(W_{max,B}\right)^2 + \left(W_{q\,max,B}\right)^2} \end{aligned} \tag{10}$$

where $P_{max,B}$ and $Q_{max,B}$ are the maximum active and reactive powers of BESS. Also, $W_{max,B}$ and $W_{q_{max,B}}$ are the maximum active and reactive energy capacity of BESS. $W_{q_{max,B}}$ is calculated as the sum of hourly reactive power.

F. Multi-objective function

The Multi-objective function consists of economic, environmental, and technical objectives as shown in (11)-(13).

$$max \sum_{l=1}^{N} \left(\left(\begin{array}{c} \left(ARB_{BEN} + TRANS_{BEN}\right) 250 \\ -C_{O\&M\&REP} \end{array} \right) \left(\frac{1+ir}{1+dr}\right)^l \right) - C_{RES\&BESS} \tag{11}$$

$$Environmental\ Objective\ Function:\ max\left(ENV_{OBJ}\right) \tag{12}$$

$$Technical\ Objective\ Function:\ max\left(LOSS_{OBJ}\right) \tag{13}$$

where N is the number of planning years whereas ir and dr are inflation and discount rates, respectively. In economic objective, operating days of RES and BESS are equal to 250 according to working days (five working days in a week, and about 10 national holidays).

The economic function is based on the net present value.

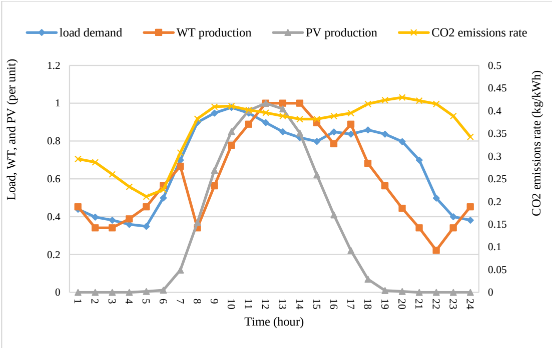

Fig. 1. The average hourly curve for load demand, power production of the WT, and the PV and average hourly CO_2 emission.

G. Constraints

Constraints include BESS and technical constraints. BESS constraints are introduced with respect to balance between charge and discharge of the BESS as shown in (14) and maximum BESS power and energy that can be expressed as (15) and (16), respectively.

$$\sum_{i=1}^{24} \left(P_i^+ - P_i^- \eta_{ESS}\right) = 0 \quad \textbf{(14)}$$

$$0 \le P_i^- \le P_{max,B} \qquad 0 \le P_i^+ \le P_{max,B} \quad \textbf{(15)}$$

$$\sum_{i=1}^{24} P_i^+ \le W_{max,B} \quad \textbf{(16)}$$

where η_{ESS} shows the BESS efficiency. To consider BESS efficiency properly, the discharging power should be lower than charging power. By applying BESS efficiency to only the power charge cycle, the discharging power is lower than charging power in each hour and thus, in a day.

In the present paper, it is assumed that the power of each hour is constant along one hour. Therefore, energy (multiplying power and one hour) is equal to power for each hour.

Technical constraints consist of bus voltage magnitude limit and prohibition of reverse power flows to the transmission network. Reverse power flows may lead to over-voltage and/or blinding of protection and false tripping. Reverse power flow is evaluated in the network by upstream line phase angle of complex power. When this angle is between 90° to 270°, power flow is reversed to the transmission network.

3. SOLUTION APPROACH

The average hourly curve for load demand [34], power production of the WT [35], and PV [34] per unit, and average hourly CO_2 emission rate [32] are shown in Fig. 1.

Active and reactive powers of buses are multiplied in the load demand profile of Fig. 1 to represent hourly load demand. The maximum powers of WTs and PVs that are calculated by optimization are multiplied respectively in hourly WT and PV production as Fig. 1 to calculate hourly power production.

The flowchart of the optimization approach is introduced in Fig. 2.

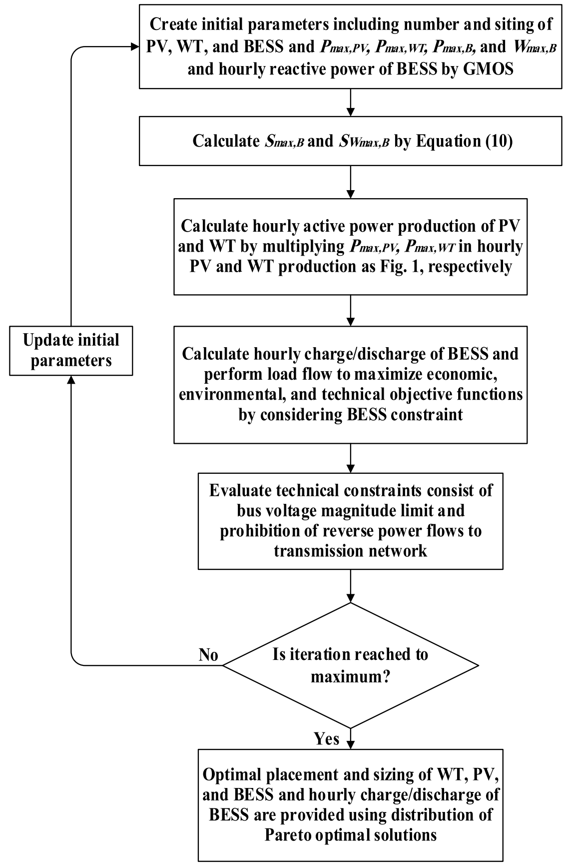

Fig. 2. Flowchart of optimization.

In the first step of this optimization approach, initial parameters including number and place of PV, WT, and BESS, $P_{max,PV}$, $P_{max,WT}$, $P_{max,B}$, $W_{max,B}$, and hourly reactive power of BESS are generated by GMOS. In the second stage, the $S_{max,B}$ and $S_{W_{max,B}}$ are calculated by (10). In the third stage, hourly active power productions of PV and WT are calculated by multiplying $P_{max,PV}$, $P_{max,WT}$ in hourly PV and WT productions of Fig. 1, respectively.

In the fourth stage, the hourly charge/discharge of BESS is calculated and load flow is performed to maximize economic, environmental, and technical objective functions. To maximize economic objective function and calculate hourly charge/discharge of BESS, linear programming is used by considering BESS constraint. In this linear programming, the interior-point algorithm has been used for optimization.

In the fifth stage, technical constraints consisting of bus voltage magnitude limit and prohibition of reverse power flows to transmission network are evaluated. If the constraints are met, the answer is stored as one of the feasible solutions. The convergence criterion is maximum iteration of GMOS assumed equal to 30. When the maximum iteration is reached, optimal placement and sizing of WT, PV, and BESS and hourly charge/discharge of BESS are provided using distribution of Pareto optimal solutions.

In the present paper, according to the flowchart of optimization, the initial (maximum) value of parameters is updated and optimized by GMOS. Therefore, the maximum value of the parameters is their optimal value.

Table 1. Data for optimization

Cost of battery and power electronic ($/kW)	$C_{S,B}$	$C_{WS,B}$	$C_{Mf_B} + C_{Mv_B}$
	426	100	9
WT cost ($/kW)	$C_{S,WT}$	$C_{Mf\,WT} + C_{Mv\,WT} + C_{REP_{COST},WT}$	
	3751	31	
PV cost ($/kW)	$C_{S,PV}$	$C_{Mf\,PV} + C_{Mv\,PV} + C_{REP_{COST},PV}$	
	2493	19	
Planning years	20		
Number of operation days in a year	250		
BESS efficiency (%)	75		
Inflation rate (%)	1.5		
Discount rate (%)	9		

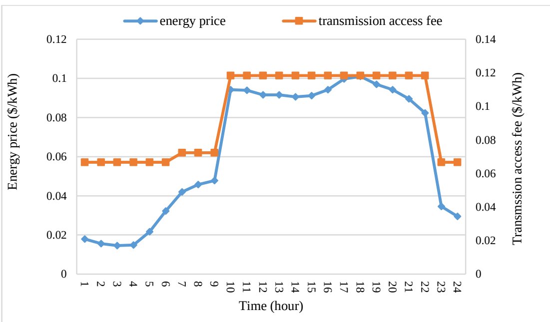

Fig. 3. Average hourly transmission access fee and energy price.

4. RESULTS

The case study includes IEEE 33-bus system, which is a radial distribution network. All loads data, resistance, and reactance of this system can be found in [36]. A backward/ forward sweep algorithm has been used for load flow and executed in MATLAB. In this paper, the optimization is performed for a 24-hour period. GMOS with linear programming is used for optimization.

In this paper, the vanadium redox flow battery energy storage system is chosen as a test example. Vanadium redox flow battery is suitable for small and medium-scale applications and its power rating depends on flow reactants and the area of the membranes, whereas the electrolyte tank capacity defines the total stored energy [37, 38].

Costs of battery [31], WT, and PV [39] (including power electronic converters), number of planning years, number of operation days in a year, BESS system efficiency, as well as inflation and discount rates [31] are assumed as Table 1.

The average hourly transmission access fee and energy price [31] are shown in Fig. 3.

In Fig. 4, the voltage magnitude of some buses before the optimization is shown.

It can be seen that in the buses far from the distribution transformer, by increasing load demand, voltage magnitude goes below the allowable limit (±5%). Also, bus 18 experiences the most sever under-voltage because this bus is the furthest bus from the distribution transformer. Under-voltage can be mitigated by the optimization of RES and BESS.

The Pareto optimal solution set of optimization RES and BESS is shown in Fig. 5.

It can be seen that by increasing economic benefit and decreasing environmental emission, energy losses increase. In the following, the reason for this issue is introduced with Figs. 6-8.

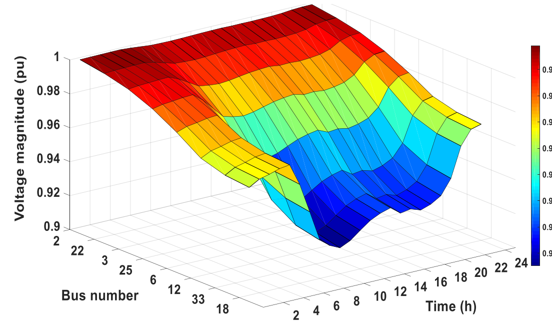

Fig. 4. Voltage magnitude before optimization.

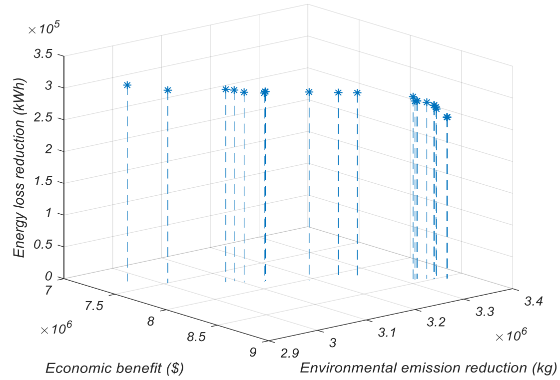

Fig. 5. Distribution of Pareto optimal solutions.

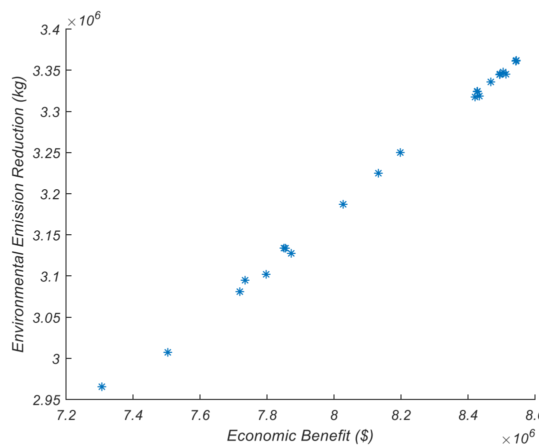

Fig. 6. Distribution of Pareto optimal solutions for environmental emission reduction and economic benefit.

In Fig. 6, the Pareto optimal solutions for economic benefit and yearly environmental emission reduction is indicated.

Numerical results show that if the economic benefit is increased, environmental emission is decreased. Economic (energy arbitrage and transmission access fee) benefit is maximized by increasing hourly energy production of RES with zero-emission rate, which leads to decreased environmental emission. On the other hand, by comparing Figs. 1-3, it is observed that when the energy price and transmission access fee are minimal, CO_2

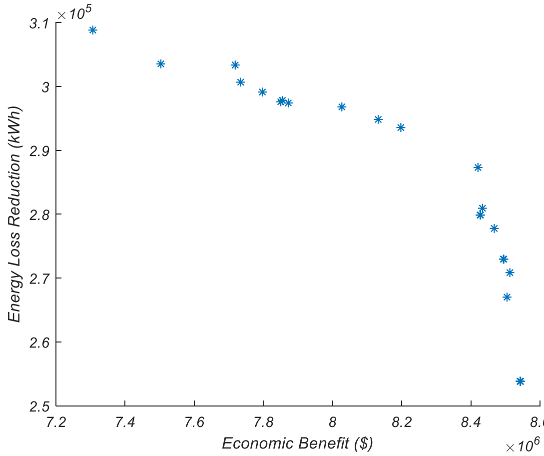

Fig. 7. Distribution of Pareto optimal solutions for energy loss reduction and economic benefit.

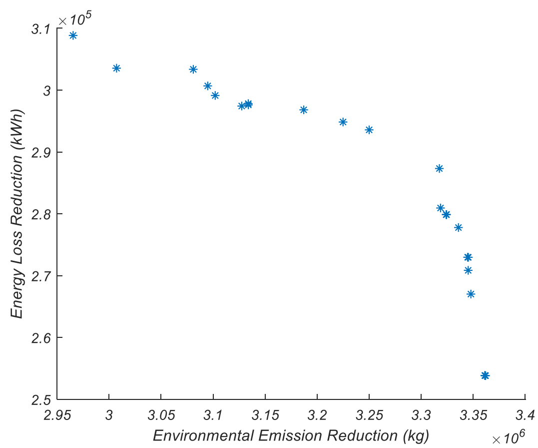

Fig. 8. Distribution of Pareto optimal solutions for energy loss and environmental emission reduction.

emission rate is approximately minimal. When the energy price and transmission access fee increase, CO_2 emission rate also grows. Therefore, to increase economic benefit and decrease environmental emission simultaneously, BESS could be charged and discharged when energy price, transmission access fee, and CO_2 emission rate are low and high, respectively.

In Figs. 7 and 8, the Pareto optimal solutions for yearly energy loss reduction with economic benefit and yearly environmental emission reduction are shown, respectively.

According to Figs. 7 and 8, when the economic benefit is increased or environmental emission is decreased, energy losses are increased. Economic and emission objectives are improved by increasing hourly energy production of RES, which leads to increased power losses because of extra energy production and reverse power flow.

In Table 2, for a set of typical solutions, the optimal placement and sizing of WT, PV, and BESS, economic benefit, yearly reduction of CO_2 emission, and yearly average reduction of losses are shown.

As can be seen in Table 2, Solution A maximizes economic benefit and minimizes environmental emission. On the other

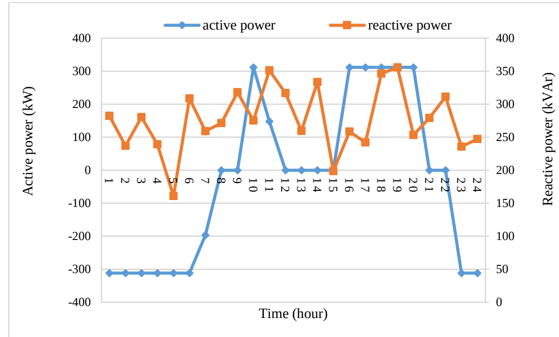

Fig. 9. Optimal scheduling of charge and discharge and reactive power production of BESS.

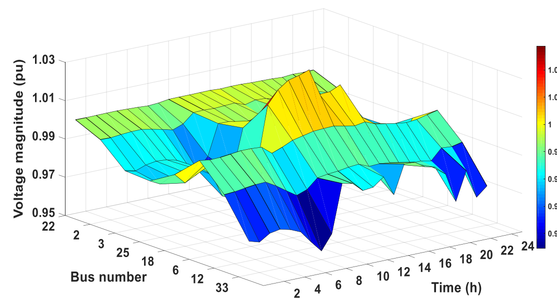

Fig. 10. Voltage magnitude after optimization.

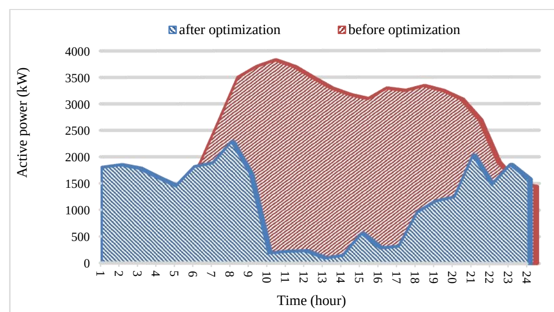

Fig. 11. Power imported from distribution transformer.

hand, Solution B minimizes energy loss. Therefore, economic benefit, CO_2 emission reduction, and energy loss in Solution A are higher than Solution B.

Optimal scheduling of BESS charge and discharge and reactive power production that is expressed by multi-objective optimization for Solution A is shown in Fig. 9.

According to Fig. 9, BESS is charged when the price of energy, transmission access fee, and CO_2 emission rate are low and discharged when these rates are high (see Figs. 1-3).

Hourly voltage magnitudes of some buses after the optimization of WT, PV, and BESS in Solution A are shown in Fig. 10.

According to Fig. 10, hourly voltage magnitudes of all buses are in allowable range after optimal planning and operation. For instance, since one of the optimally rated WTs is placed on bus 18, under-voltage of this bus is improved.

In Fig. 11, power imported from distribution transformer for Solution A is shown.

As can be seen in Fig. 11, in total, DSO can buy lower en-

Table 2. Optimal optimization solution

	WT Node & Sizing (kW)	PV Node & Sizing (kW)	BESS Node & Sizing (kW) & (kWh)	Economic Benefit $\times 10^6$ (\$)	Reduction of CO_2 emission $\times 10^6 (kg)$	Average reducing losses $\times 10^5$ (kWh)
Solution A	18, 22, 29 & 396, 888, 505	17, 23, 28 & 764, 335, 262	8, 28, 30 & 312 & 2018	8.5439	3.3619	2.5375
Solution B	17, 28 & 645, 805	16, 21, 25 & 709, 278, 256	6, 28, 30 & 313 & 1896	7.3067	2.9655	3.0875

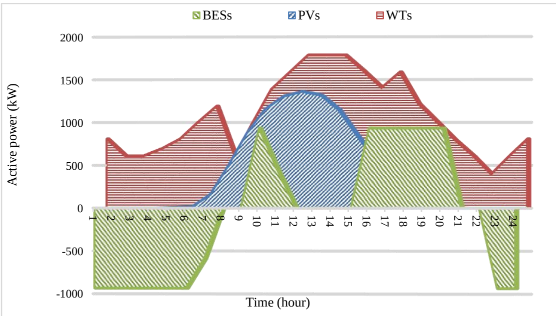

Fig. 12. The average hourly energy production.

ergy from the power market (through the transmission system) because of optimization. During midnight, imported power is increased because of BESS charging suggested by the optimization algorithm. On the other hand, in the rest of the day imported power is decreased due to WT and PV production and BESS discharging. Also, the proposed optimization prevented reverse power flow to the transmission network.

Fig. 12 shows the average hourly energy production of WTs, PVs, and BESS only in Solution A.

As mentioned before, to increase economic and decrease environmental emission, BESS can charge at midnight. To decrease purchasing energy from the power market in this period, proper WT units are planned in the network. Therefore, the maximum power of WTs is higher than PVs, however the capital and maintenance costs of PV are lower than WT (see Tables 1 and 2).

5. CONCLUSION

In this paper, optimal placement, sizing, and operation of RES and BESS were performed according to economic, environmental, and technical objectives by using a multi-objective function. Optimal simultaneous planning and operation were performed using a multi-objective function and linear programming, respectively. The effectiveness of the optimization was tested with a comprehensive case study on IEEE 33 bus test system. It was indicated that increasing economic benefit had reduced environmental emission and increased energy losses. It was concluded that although the capital cost of RES and BESS installing is high, an acceptable economic benefit could be obtained through proper planning and operation. For this purpose, BESS is charged when the energy price, transmission access fee, and CO_2 emission rate are low and discharged when these rates are high. In addition, environmental emission and energy losses were decreased. Moreover, hourly voltage magnitudes of all buses were in allowable range and reverse power flow was prevented.

In this paper, the uncertain nature of PV and WT is not taken into account. In addition, the average hourly load demand was applied instead of different hourly load demand for each day. These issues can be addressed in future studies by considering probabilistic optimization.

REFERENCES

1. N. T. Kalantari, M. A. Hassas, and K. Pourhossein, "Bibliographic review and comparison of optimal sizing methods for hybrid renewable energy systems," Journal of Energy Management and Technology, vol. 2, no. 2, pp. 66-79, 2018.
2. C. Brivio, S. Mandelli, and M. Merlo, "Battery energy storage system for primary control reserve and energy arbitrage," Sustainable Energy Grids and Networks, vol. 6, pp. 152-165, 2016.
3. M. Hosseina and S. M. T. Bathaee, "Optimal scheduling for distribution network with redox flow battery storage," Energy Conversion and Management, vol. 121, pp. 145-151, 2016.
4. B. Li, X. Li, X. Bai, and Z. Li, "Storage capacity allocation strategy for distribution network with distributed photovoltaic generators," Journal of Modern Power Systems and Clean Energy, vol. 6, no. 6, pp. 1234-1243, 2018.
5. T. Khatib, I. A. Ibrahim, and A. Mohamed, "Review on sizing methodologies of photovoltaic array and storage battery in a standalone photovoltaic system," Energy Conversion and Management, vol. 120, pp. 430-448, 2016.
6. C. Sabillon, J. F. Franco, M. J. Rider, and R. Romero, "Joint optimal operation of photovoltaic units and electric vehicles in residential networks with storage systems: a dynamic scheduling method," International Journal of Electrical Power & Energy Systems, vol. 103, pp. 136-145, 2018.
7. K. Kusakana, "Optimal scheduling for distributed hybrid system with pumped hydro storage," Energy Conversion and Management, vol. 111, pp. 253-260, 2016.
8. S. R. Ghatak, S. Sannigrahi, and P. Acharjee, "Optimised planning of distribution network with photovoltaic system, battery storage, and DSTATCOM," IET Renewable Power Generation, vol. 12, no. 15, pp. 1823-1832, 2018.
9. V. Kalkhambkar, R. Kumar, and R. Bhakar, "Joint optimal allocation methodology for renewable distributed generation and energy storage for economic benefits," IET Renewable Power Generation, vol. 10, no. 9, pp. 1422-1429, 2016.
10. J. Qiu, Z. Xu, Y. Zheng, D. Wang, and Z. Y. Dong, "Distributed generation and energy storage system planning for a distribution system operator," IET Renewable Power Generation, vol. 12, no. 12, pp. 1345-1353, 2018.
11. M. Sedighizadeh, A. H. Mohammadpour, and S. M. M. Alavi, "A two-stage optimal energy management by using ADP and HBB-BC algorithms for microgrids with renewable energy sources and storages," Journal of Energy Storage, vol. 21, pp. 460-480, 2019.
12. O. Talent and H. Du, "Optimal sizing and energy scheduling of photovoltaic-battery systems under different tariff structure," Renewable Energy, vol. 129, pp. 513-526, 2018.
13. K. Anoune, A. Laknizi, M. Bouya, A. Astito, and A. B. Abdellah, "Sizing a PV-Wind based hybrid system using deterministic approach," Energy Conversion and Management, vol. 169, pp. 137-148, 2018.
14. H. Bakhtiari and R. A. Naghizadeh, "Multi-criteria optimal sizing of hybrid renewable energy systems including wind, photovoltaic, battery, and hydrogen storage with ε-constraint method," IET Renewable Power Generation, vol. 12, no. 8, pp. 883-892, 2018.
15. H. Saboori and R. Hemmati, "Maximizing DISCO profit in active distribution networks by optimal planning of energy storage systems and distributed generators," Renewable and Sustainable Energy Reviews, vol. 71, pp. 365-372, 2017.
16. J. Salehi, S. Esmaeilpour, F. S. Gazijahani, and A. Safari, "Risk based battery energy storage and wind turbine allocation in distribution networks using fuzzy modeling," Journal of Energy Management and

Technology, vol. 2, no. 2, pp. 53-65, 2018.
17. S. Mahdavi, R. Hemmati, and M. A. Jirdehi, "Two-level planning for coordination of energy storage systems and wind-solar-diesel units in active distribution networks," Energy, vol. 151, pp. 954-965, 2018.
18. M. Ban, J. Yu, M. Shahidehpour, and D. Guo, "Optimal sizing of PV and battery-based energy storage in an offgrid nanogrid supplying batteries to a battery swapping station," Journal of Modern Power Systems and Clean Energy, vol. 7, no. 2, pp. 309-320, 2019.
19. M. R. Jannesar, A. Sedighi, M. Savaghebi, and J. M. Guerrero, "Optimal placement, sizing, and daily charge/discharge of battery energy storage in low voltage distribution network with high photovoltaic penetration," Applied Energy, vol. 226, pp. 957-966, 2018.
20. M. Vatanpour and A. S. Yazdankhah, "Application of Benders decomposition in stochastic scheduling of thermal units with coordination of wind farm and energy storage system considering security constraint," Journal of Energy Management and Technology, vol. 2, no. 1, pp. 9-17, 2018.
21. J. Salehi, S. Esmaeilpour, A. Safari, and F. Samadi, "Investment deferral of sub-transmission substation using optimal planning of wind generators and storage systems," Journal of Energy Management and Technology, vol. 1, no. 1, pp. 18-29, 2017.
22. O. Erdinc, A. Taşcıkaraoglu, N. G. Paterakis, I. Dursun, M. C. Sinim, and J. P. S. Catalao, "Comprehensive optimization model for sizing and siting of DG units, EV charging stations, and energy storage systems," IEEE Transactions on Smart Grid, vol. 9, no. 4, pp. 3871-3882, 2018.
23. K. K. Mehmood, S. U. Khan, S. Lee, Z. M. Haider, M. K. Rafique, and C. Kim, "Optimal sizing and allocation of battery energy storage systems with wind and solar power DGs in a distribution network for voltage regulation considering the lifespan of batteries," IET Renewable Power Generation, vol. 11, no. 10, pp. 1305-1315, 2017.
24. A. Abbassi, R. Abbassi, M. A. Dami, and M. Jemli, "Multi-objective genetic algorithm based sizing optimization of a stand-alone wind/PV power supply system with enhanced battery/supercapacitor hybrid energy storage," Energy, vol. 163, pp. 351-363, 2018.
25. M. Ahmadi, M. E. Lotfy, M. S. S. Danish, S. Ryuto, A. Yona, and T. Senjyu, "Optimal multi-configuration and allocation of SVR, capacitor, centralised wind farm, and energy storage system: a multi-objective approach in a real distribution network," IET Renewable Power Generation, vol. 13, no. 5, pp. 762-773, 2019.
26. J. Duchaud, G. Notton, C. Darras, and C. Voyant, "Multi-objective Particle Swarm optimal sizing of a renewable hybrid power plant with storage," Renewable Energy, vol. 131, pp. 1156-1167, 2019.
27. Y. Zhang, A. Lundblad, P. E. Campana, F. Benavente, and J. Yan, "Battery sizing and rule-based operation of grid-connected photovoltaic-battery system: a case study in Sweden," Energy Conversion and Management, vol. 133, pp. 249-263, 2017.
28. M. Javidsharifi, T. Niknam, J. Aghaei, and G. Mokryani, "Multi-objective short-term scheduling of a renewable-based microgrid in the presence of tidal resources and storage devices," Applied Energy, vol. 216, pp. 367-381, 2018.
29. Y. Sawle, S. C. Gupta, and A. K. Bohre, "Socio-techno-economic design of hybrid renewable energy system using optimization techniques," Renewable Energy, vol. 119, pp. 459-472, 2018.
30. A. Belderbos, A. Virag, W. D'haeseleer, and E. Delarue, "Considerations on the need for electricity storage requirements: power versus energy," Energy Conversion and Management, vol. 143, pp. 137-149, 2017.
31. R. C. Leou, "An economic analysis model for the energy storage system applied to a distribution substation," International Journal of Electrical Power & Energy Systems, vol. 34, no. 1, pp. 132-137, 2012.
32. A. Talaei, K. Begg, and T. Jamasb, "The large scale roll-out of electric vehicles: the effect on the electricity sector and CO2 emissions," EPRG Working Paper 1222, 2012.
33. H. Chen, T. N. Cong, W. Yang, C. Tan, Y. Li, and Y. Ding, "Progress in electrical energy storage system: a critical review," Progress in Natural Science, vol. 19, no. 3, pp. 291-312, 2009.
34. G. Carpinelli, G. Celli, S. Mocci, F. Mottola, F. Pilo, and D. Proto, "Optimal integration of distributed energy storage devices in smart grids," IEEE Transactions on Smart Grid, vol. 4, no. 2, pp. 985-995, 2013.
35. S. X. Chen, H. B. Gooi, and M. Q. Wang, "Sizing of energy storage for microgrids," IEEE Transactions on Smart Grid, vol. 3, no. 1, pp. 142-151, 2012.
36. A. D. Rana, J. B. Darji, and M. Pandya, "Backward/Forward sweep load flow algorithm for radial distribution system," International Journal for Scientific Research & Development, vol. 2, pp. 398-400, 2014.
37. O. M. Toledo, D. O. Filho, and A. S. A. C. Diniz, "Distributed photovoltaic generation and energy storage systems: a review," Renewable and Sustainable Energy Reviews, vol. 14, no. 1, pp. 506-511, 2010.
38. F. D. González, A. Sumper, O. G. Bellmunt, and R. V. Robles, "A review of energy storage technologies for wind power applications," Renewable and Sustainable Energy Reviews, vol. 16, no. 4, pp. 2154-2171, 2012.
39. "Electricity cost from renewable energy technologies in Egypt," Fraunhofer Institute for Solar Energy System ISE, 2016.